

Automatic Calibration of Low Cost Inertial Gyroscopes with a PTU

Delgado. J.V., Silva. P. R. M., Quiroz. C.H.C. and, Kurka, P.R.G.*

Abstract—This work proposes a low cost calibration method for micro-electro-mechanical inertial (MEMS) gyroscopes, using a camera pan-tilt base. The use of MEMS gyroscopes in practical robotics measurements requires preliminary calibration. Three calibration procedures are currently found in the literature to estimate the sensor calibration parameters which are based on static, quasi-static and dynamic measurements. This paper focus in the investigation of quasi-static calibration procedure which consists in moving the sensor in a path with known kinematics. High complexity calibration mechanisms were proposed in the literature, which require user intervention. This paper proposes a simple procedure to calibrate a gyroscope using an automatic camera pan tilt base. The sensor parameters are estimated using direct pseudo inversion of a coefficients matrix. The method is validated experimentally on two different IMU platforms.

Key words—Calibration, IMU, Gyroscope.

I. INTRODUCTION

Inertial measurements units (IMU's) have been used as instruments to assess movement in industrial and robotic applications. Three different sensors comprise a typical IMU; accelerometers, magnetometers and gyroscopes. The application of IMU in intelligent transportation systems (ITSC) has been growing steadily. In 1997, micro-electro-mechanical systems (MEMS) were used in military applications and later into the automotive industry. The work of N.Barbour [1] introduces the use of silicon micromechanical gyroscopes and accelerometers in automotive system applications such as deploying air bags, control of vehicle suspension, wheel steering, breaking and engine diagnostics and also augmenting the GPS and map display data for navigation. The work of R. Carballedo [2] presents a railway localization system using GPS, maps and three orthogonal lineal accelerometers and gyroscopes. Heirich [3] presents a measurement and analysis of train motion using an IMU.

The production of IMU's has grown alongside the development of MEMS. Researchers say that "although MEMS sensors are mass-produced by a same process, each sensor unit has its own characteristics" [4]. Manufacturers datasheet say that IMU's are stable over time and temperature.

*Research supported by, CNPq, CAPES and FAPEAM Foundations.

Delgado, J.V. is with the "Faculdade de Engenharia Mecânica", Universidade Estadual de Campinas, São Paulo, Brazil, (jaimesdelgadovargas@gmail.com).

Silva, P. R. M. and Quiroz, C.H.C. are doutoral students at the "Faculdade de Engenharia Mecânica", Universidade Estadual de Campinas, São Paulo, Brazil, (engpedroramon@gmail.com) and (cesar@fem.unicamp.br).

Kurka, P.R.G. is with the "Faculdade de Engenharia Mecânica", Universidade Estadual de Campinas, São Paulo, Brazil, (kurka@fem.unicamp.br).

Manufacturers also warn to the existence of offsets and noisy readings due to mechanical stresses of the printed circuits. Calibration is thus the solution to compensate for systematic noise and drift readings in an IMU. Researchers have been working on three procedures to estimate the sensor calibration parameters which are based on static, quasi-static and dynamic measurements[4].

Static calibration methods use the gravity and the earth rotation as references to calibrate inertial based sensors. A six-position calibration method was used in [5] to calculate inertial sensors scale factor and bias. The sensor is placed in six different positions and scale factor and bias are estimated. However the accuracy depends on the vertical axis alignment between the IMU and the frame reference [6]. Such procedures require the use of accurate mechanical platforms.

Quasi static calibration procedures also use gravity as a reference element. In such procedure, however, the IMU moves to predefined angular positions at a constant speed. The work of J. Rohac [7], proposes an inexpensive mechanical calibration platform which rotates in 3 degrees of freedom around the IMU center. Such mechanism is manually operated. The work of W. T. Fong [8] presents an IMU calibration where the IMU is rotated six times. After each rotation the IMU is manually reallocated. The work of Aggarwal [6] estimates the IMU parameters using the six positions static test and angular rate. A gyroscope and accelerometer is calibrated in a controlled room temperature (22°C). In the work of Hall [9] four pneumatic actuators control a Stewart platform to calibrate a 4 degrees of freedom (DOF) IMU. The work of D. Lee [4] uses a single axis speed rate-table to calibrate an IMU array sensor (four low cost IMU-MEMS). D. Lee's procedure requires sensor reallocation between experiments.

The present quasi static calibration methods require complex structures or user intervention. This paper proposes a simple and automatic calibration procedure using a motorized camera PTU with two DOF. Oscillation measurements around each IMU axis are recorded and compared with a reference movement. The calibration parameters are estimated using the pseudo inverse of a data matrix. Two IMU sensors were calibrated in order to validate the method, the units GY-80 [10] 10DOF and the MPU 6515 with 6DOF (gyro + accelerometer) mounted in a Nexus 5 smartphone. The GY80 sensor is used in the work of [11] which evaluates the MEMS accuracy for tracking and positioning the movement of a bike. The MPU 6515 sensor is used in the smartphone and studied by Pretto[12], which suggests that current smartphone sensors are usually poorly calibrated, resulting in measurements with non-negligible systematic and random errors. In the present work, all

sensors are attached to a pant tilt robotic arm (PTU) which oscillates continuously in preprogrammed positions.

This work is organized as follows. Section II presents the materials and methods used in the IMU calibration procedure. The experimental description and the dataset used to validate the algorithm are presented in section III. The measurement calibration parameters are validated and error is measured in section IV. Assessment of the algorithm's accuracy and final conclusions are presented in section V.

II. MATERIALS AND METHODS

This section presents the sensors and pan-tilt platform considered, the gyroscope error model, the Euler transformation algorithm and the proposed calibration method.

An MPU6515 unit, inbuilt in a Nexus 5 mobile phone and a GY80-MPU device [13] are used to validate the calibration algorithm. A pan-tilt rotation motorized platform (PTU – E46 17.5) is used to rotate the sensors around the tilt and pan axes. The PTU provides precise positioning in an extremely small and lightweight package[14]. The two low cost gyroscopes embedded in the GY80 and MPU 6515 (cellphone) units are low-power three-axes angular rate sensors with technical specifications presented the Table 1.

TABLE 1 SENSOR CHARACTERISTICS

| Parameter | GY80 (L3G4200D) | Nexus (MPU 6515) |
|-------------------------|--------------------|---------------------|
| Measurement range °/sec | ±250 | ±250 |
| Resolution | 16-bit | 16-bit |
| Sensitivity ° | 0.00875 | 0,07445 |

A. Error Model

The angular rate IMU calibration process estimates the parameters of the sensor model proposed by D. Jurman [15] as,

$$\mathbf{y} = \mathbf{S} \mathbf{T} \mathbf{M} \mathbf{u}, \quad (1)$$

where \mathbf{y} is a vector with a particular measurement of angular position of IMU gyroscopes in three different directions $[\phi \psi \theta]$. Such angular positions are calculated from the integration of unbiased angular speed measurements. The angular speed bias vector in the direction of each one of the gyroscopes of the IMU is represented as,

$$\mathbf{b} = [b_x \ b_y \ b_z]^T. \quad (2)$$

The vector of reference angles in three orthogonal positions $[\theta_x \theta_y \theta_z]$ is described as \mathbf{u} . The scale \mathbf{S} and orthogonality calibration matrix \mathbf{T} , which transforms the orthogonal coordinates system into a non-orthogonal one, are given respectively by,

$$\mathbf{S} = \begin{bmatrix} S_x & 0 & 0 \\ 0 & S_y & 0 \\ 0 & 0 & S_z \end{bmatrix}, \quad (3)$$

and,

$$\mathbf{T} = \begin{bmatrix} 1 & 0 & 0 \\ \alpha_{xy} & 1 & 0 \\ \alpha_{zx} & \alpha_{zy} & 1 \end{bmatrix}. \quad (4)$$

Deformation parameters between the expected and IMU measurement frames comprise the elements of the misalignment matrix,

$$\mathbf{M} = \begin{bmatrix} m_{xx} & m_{xy} & m_{xz} \\ m_{xy} & m_{yy} & m_{yz} \\ m_{zy} & m_{zy} & m_{zz} \end{bmatrix}. \quad (5)$$

B. Proposed Calibration algorithm

The calibration algorithm uses the PTU as a reference to calibrate the gyroscope. Oscillations around each IMU axis are converted into Euler angles, recorded and compared with pan-tilt angles. The procedure is illustrated in Fig. 1. Rotations around the pan tilt angles of the mechanism are projected through Euler rotations into the frame of measured angular positions of the sensors.

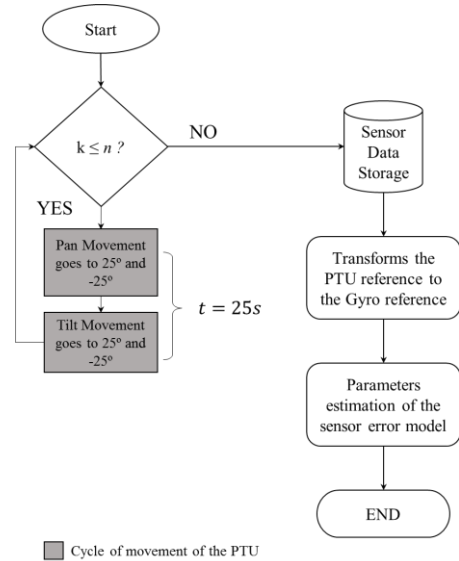


Fig. 1 Calibration procedure, the PTU follows the calibration path in the pan and tilt movements. Gyroscope dates is recorded and parameters are subsequently estimated.

The process starts with a pan movement followed by a tilt rotation. The cycle is repeated n times, while the sensor angles and PTU references are being continuously recorded. The data is subsequently processed leading to the estimates of the gyroscope calibration parameters.

The proposed calibration method stores all gyroscope measurements and PTU references in matrices of vectors $\mathbf{Y} = [\mathbf{y}_1 \ \mathbf{y}_2 \ \dots \ \mathbf{y}_n]$ and $\mathbf{U} = [\mathbf{u}_1 \ \mathbf{u}_2 \ \dots \ \mathbf{u}_n]$, respectively. Vectors \mathbf{y}_k and \mathbf{u}_k have the instantaneous measurements of the gyroscopic axis rotations and known PTU instantaneous attitude angles represented respectively as,

$$y_k = \begin{bmatrix} \theta_x \\ \theta_y \\ \theta_z \end{bmatrix} \quad \text{and} \quad u_k = \begin{bmatrix} \phi \\ \psi \\ \theta \end{bmatrix} \quad (6)$$

The implicit calibration parameters in the **STM** matrix are calculated by,

$$\mathbf{STM} = \mathbf{YU}^+, \quad (7)$$

where the symbol $+$ represents the pseudoinverse operation. Cholesky (*chol*) decomposition is used to extract the lower triangular matrix product **ST**.

$$\mathbf{ST} = \text{chol}[\mathbf{STM} \mathbf{STM}^T]^T \quad (8)$$

Matrices **S** and **T** can be readily obtained through the “Lower Upper” (*LU*) factorization applied to **ST** that is,

$$[\mathbf{S}, \mathbf{T}] = \text{LU}(\mathbf{ST}) \quad (9)$$

Matrix **M** is thus calculated as,

$$\mathbf{M} = \mathbf{T}^{-1} \mathbf{S}^{-1} \mathbf{STM} \quad (10)$$

C. Euler transformation angles

The PTU rotations around the *Pan* and *Tilt* axes are represented by Euler angles (φ, ψ, θ) as illustrated in Fig2.

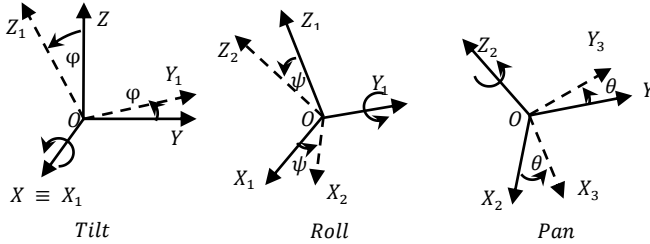


Fig. 2 PTU reference to Euler IMU angles.

The transformation from PTU angles to gyroscope Euler angles is defined as,

$$\begin{bmatrix} \psi_k \\ \phi_k \\ \theta_k \end{bmatrix} = \begin{bmatrix} \text{atan}(\mathbf{R}_t(3,2)_k, \mathbf{R}_t(3,3)_k) \\ \text{atan}\left(\frac{\mathbf{R}_t(2,1)_k}{\cos(\theta_k)}, \frac{\mathbf{R}_t(1,1)_k}{\cos(\theta_k)}\right) \\ -\sin^{-1}(\mathbf{R}_t(3,1)_k) \end{bmatrix} \quad (11)$$

where the cumulative rotation matrix \mathbf{R}_t is updated at each step with the axes rotations matrices R_x , R_y and R_z defined as,

$$\mathbf{R}_{t(k)} = \mathbf{R}_z(\Delta Pan) \cdot \mathbf{R}_y(\Delta Roll) \cdot \mathbf{R}_x(\Delta Tilt) \cdot \mathbf{R}_{t(k-1)}. \quad (12)$$

III. EXPERIMENTAL SETUP

The PTU unit is used to move the IMU's in predefined angular orientations. Rotations in the Pan and Tilt directions are recorded together with corresponding gyroscope measurements. Two calibration experiments are performed in this work. Firstly, a static test of the IMU was carried out with zero initial Pan and Tilt angles, as presented in the Fig.

3(b). Data was recorded during 100 seconds and used to estimate the calibration parameters associated with inherent noise and offset of the units.

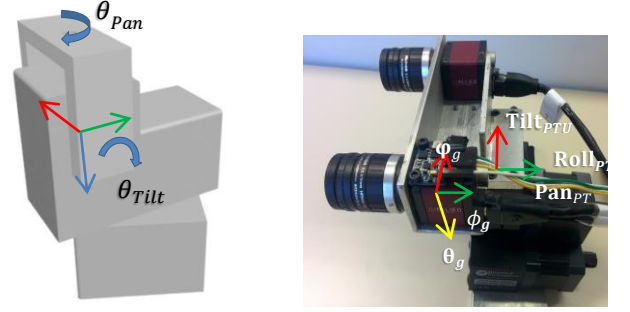


Fig. 3 (a) Pan-Tilt rotations. (b) IMU GY80 fixed in the PTU.

In the second test, the PTU moves in the predefined pattern presented in Fig4b. It starts with a rotation around the pan angle. Then, it moves around the tilt direction. Such a cycle is repeated in four periods, totaling 75s, as show in Fig. 4b. Transformed PTU reference rotation angles and sensor measurements allow the calculation of the calibration parameters according to the procedure described in section II.C. The converted angles (φ, ϕ, θ) are illustrated in Fig. 4a.

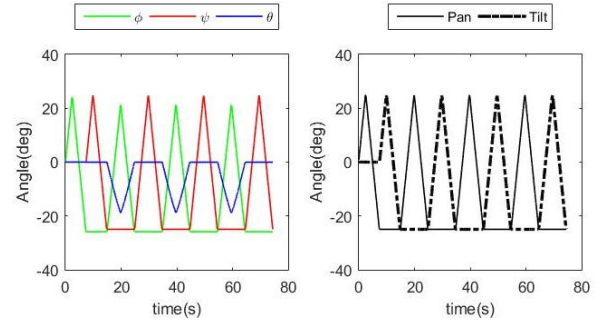


Fig. 4 (a) Reference path angles in Euler angles. (b) Reference PTU angles.

The sensors measurements were all recorded and synchronized with the PTU data. Two data-sets were recorded in order to calibrate the IMUs. First, a Java application was developed to extract the angular velocities of the sensor (MPU 6515). Such data was stored internally in a text file with time stamps. The GY 80 sensor measurements were transmitted via RS232 protocol to an external computer and stored with time stamps in a text file. Such an acquisition procedure was developed in C++ . Finally, calibration was implemented in Matlab. The results of such an implementation are shown in section IV.

IV. RESULTS

Experimental calibration results are separately presented in the sequence, for the GY80 and the cellphone IMU's.

A. Gyroscope GY80:

The bias was calculated for each one of the three gyro sensor angles, using the measurements of the static test. Integration drift is represented in Fig5(a), and the primitive

bias estimated through calculation of the angular coefficients of the interpolating lines. Fig5(b) presents the integrated gyro signals after correction with the estimated bias values.

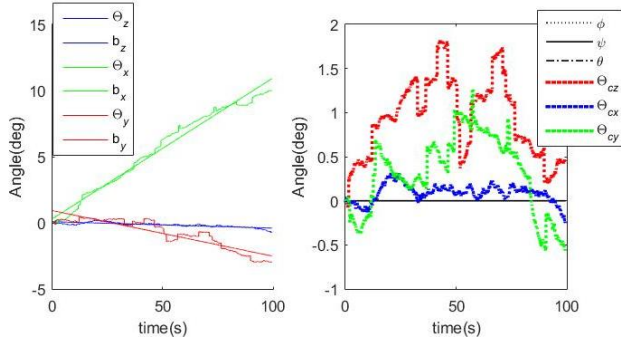


Fig.5 (a) Measure angles of static experiment with Gyroscope GY80. (b) Measurements without bias.

Quasi static calibration test data is shown in Fig6(a) displaying the three integrated gyroscope signals with their inherent drift. Bias is estimated and represented through the continuous lines for each sensor axis measurement. Fig6(b) displays the integrated results of bias compensated measurements.

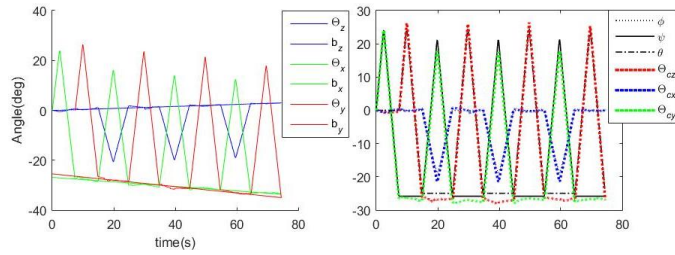


Fig. 6 (a) Bias estimation of quasi static test and (b) measurements without bias using Gyroscope GY80.

Estimation of resulting static and quasi static bias parameters and calibration matrices are presented in Table II below.

Table 2 Bias error

| Test | GY80 (L3G4200D) | Nexus (MPU 6515) |
|--------------|--------------------------|---------------------------|
| Static | [0.106 - 0.004 - 0.034] | [0.0135 0.0258 0.0074] |
| Quasi static | [-0.090 0.040 - 0.127] | [0.0327 - 0.0021 0.0300] |

The calibration parameters are now used to compare the angles measured by the gyroscopic sensors and the reference pan tilt unit. Fig7 (a) shows the pant tilt quasi static test angles, compared to the equivalent angular measurements made with uncalibrated sensors. Fig7 (b) shows the same comparison using calibrated sensor signals.

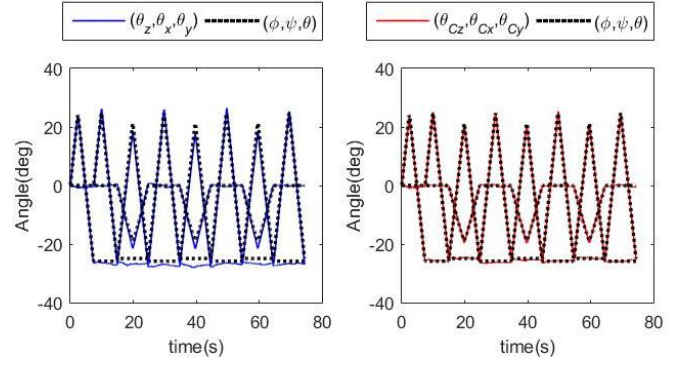


Fig. 7 (a) Uncalibrated measurements of Gyroscope GY80 and the corrected signal (b).

B. Cellphone: MPU 6515

The calibration algorithm is tested with a cellphone IMU. The bias is calculated for each angular position using the measurements of static test for 30 seconds. The estimated bias and the corrected angular speed are presented in Fig8.

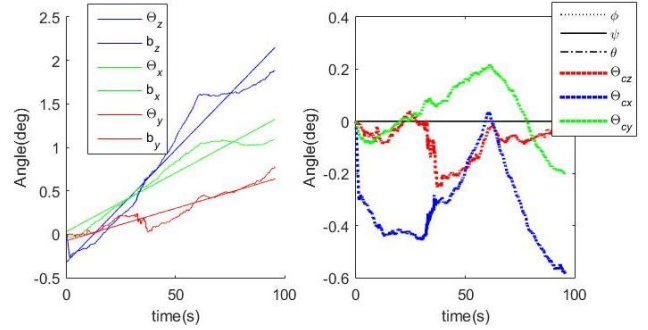


Fig. 8 (a) Uncalibrated measurements of MPU6515 and the corrected signal (b).

The quasi static calibration test is presented in Fig9. The measured bias is represented by a continuous line. Fig9. displays the results of bias being extracted from the signal.

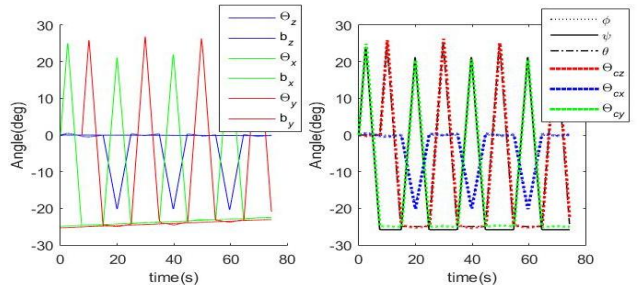


Fig. 9 (a) Bias estimation of quasi static test and (b) measurements without bias using Gyroscope 6515

Fig10 (a) shows, the measurements made with uncalibrated sensors in a quasi static test, and its comparison with the reference signal. The equivalent calibrated angles are presented in Fig10 (b).

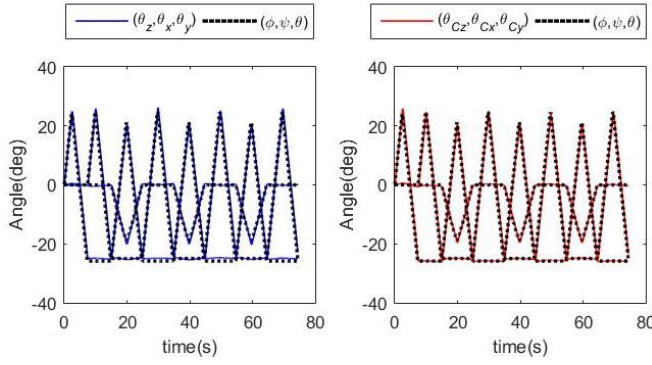


Fig. 10 (a) Uncalibrated measurements of MPU6515 and the corrected signal (b).

The estimated calibration parameters are shown in Table 3 below. Estimates of matrices \mathbf{T} and \mathbf{M} have different signals since the sensors have different positive directions of the z axis.

TABLE 3 STM PARAMETERS

| | GY80 | MPU 6515 |
|--------------|---|---|
| \mathbf{S} | $\begin{bmatrix} 0.9482 & 0 & 0 \\ 0 & 0.9734 & 0 \\ 0 & 0 & 0.8854 \end{bmatrix}$ | $\begin{bmatrix} 0.9865 & 0 & 0 \\ 0 & 1.0352 & 0 \\ 0 & 0 & 0.9517 \end{bmatrix}$ |
| \mathbf{T} | $\begin{bmatrix} 1 & 0 & 0 \\ -0.0155 & 1 & 0 \\ -0.0312 & -0.1504 & 1 \end{bmatrix}$ | $\begin{bmatrix} 1 & 0 & 0 \\ 0.0359 & 1 & 0 \\ 0.0481 & 0.0321 & 1 \end{bmatrix}$ |
| \mathbf{M} | $\begin{bmatrix} 0.9988 & -0.0078 & -0.0481 \\ 0.0004 & 0.9883 & -0.1524 \\ 0.0487 & 0.1522 & 0.9871 \end{bmatrix}$ | $\begin{bmatrix} 0.9989 & 0.0351 & 0.0313 \\ -0.0106 & 0.9885 & 0.0309 \\ -0.0302 & -0.0320 & 0.9990 \end{bmatrix}$ |

The temperature variations were not taken into account in this paper. Android and IMU gyroscope readings had temperature compensation, according to the manufacturer. Interesting discussions about bias drift, angular velocity and orientation errors due to temperature changes can be seen in the works of Feng [16] and Xia [17].

V. CONCLUSION

We have implemented a new method to calibrate a low cost gyroscope. The algebraic operations to calculate the parameters are presented and avoid traditionally heuristics procedures. The static and quasi static calibration procedures find different parameters values for the same IMU. The results suggests that the quasi static technic is more accurate than static procedure. The IMU GY80 accuracy was improved in 5.93% with the quasi static calibration. The MPU6515 was improved in 0.96%. The use of PTU as calibration tool was validated and showing the potential application.

ACKNOWLEDGMENT

The authors wish to thank the DCA laboratory, of Faculdade de Engenharia Elétrica e de Computação - UNICAMP and the Brazilian research founding agencies, FAPEAM, CNPq and CAPES, sponsors of the present work.

REFERENCES

- [1] N. Barbour, E. Brown, J. Connelly, J. Dowdle, G. Brand, J. Nelson, J. O'Bannon, J. Conneily, and J. Dowdle, "Micromachined inertial sensors for vehicles," *Intell. Transp. Syst.*, pp. 1058–1063, 1997.
- [2] R. Carballo, I. Salaberria, and A. Perallos, "Managing the Railway Traffic in Emergency Situations," *13th Int. IEEE Conf. Intell. Transp. Syst.*, pp. 285–290, 2010.
- [3] O. Heirich, A. Lehner, P. Robertson, and T. Strang, "Measurement and analysis of train motion and railway track characteristics with inertial sensors," *IEEE Conf. Intell. Transp. Syst. Proceedings, ITSC*, pp. 1995–2000, 2011.
- [4] D. Lee, S. Lee, S. Park, and S. Ko, "Test and Error Parameter Estimation for MEMS - Based Low Cost IMU Calibration," vol. 12, no. 4, pp. 597–603, 2011.
- [5] D. Titterton and J. L. Weston, *Strapdown Inertial Navigation Technology*, titterton. Peter Peregrinus Ltd, 2004.
- [6] Aggarwal, P., Syed, Z., Niu, X., and El-Sheimy, "A Standard Testing and Calibration Procedure for Low Cost MEMS Inertial Sensors and Units," *J. Navig.*, vol. 61, pp. 323–336, 2008.
- [7] J. Rohac, M. Sipos, and J. Simanek, "Calibration of Low-cost Triaxial Inertial Sensors," *IEEE Instrum. Meas. Mag.*, no. December, pp. 32–38, 2015.
- [8] W. T. Fong, S. K. Ong, and A. Y. C. Nee, "Methods for in-field user calibration of an inertial measurement unit without external equipment," vol. 19, 2008.
- [9] J. J. Hall, R. L. W. II, and F. van Graas, "Inertial Measurement Unit Calibration Platform," *J. Robot. Syst.*, no. 740, pp. 623–632, 2000.
- [10] STMicroelectronics group of companies, "MEMS motion sensor Datasheet," 2010. [Online]. Available: <http://www.st.com/web/en/resource/technical/document/datasheet/CD00265057.pdf>. [Accessed: 02-Feb-2016].
- [11] S. Miah, I. Kaparias, and P. Liatsis, "Evaluation of MEMS Sensors Accuracy for Bicycle Tracking and Positioning," pp. 299–303, 2015.
- [12] A. Pretto and G. Grisetti, "Calibration and performance evaluation of low-cost IMUs," in *18th International Workshop on ADC Modelling and Testing*, 2014.
- [13] "GY-80 - Multi Sensor Board - 3 Axis Gyro -3 Axis Accelerometer - 3 Axis Magnetometer - Barometer - Thermometer."
- [14] F. Systems, "PTU-E46 User Manual." p. 56, 2014.
- [15] D. Jurman, M. Jankovec, R. Kamnik, and M. Topič, "Calibration and data fusion solution for the miniature attitude and heading reference system," *Sensors Actuators, A Phys.*, vol. 138, no. 2, pp. 411–420, 2007.
- [16] Y. Feng, X. Li, and X. Zhang, "An adaptive compensation algorithm for temperature drift of micro-electro-mechanical systems gyroscopes using a strong tracking Kalman filter," *Sensors (Switzerland)*, vol. 15, no. 5, pp. 11222–11238, 2015.
- [17] D. Xia, S. Chen, S. Wang, and H. Li, "Microgyroscope temperature effects and compensation-control methods," *Sensors*, vol. 9, no. 10, pp. 8349–8376, 2009.